UPDATES ON BEAM SIZE MEASUREMENT USING SEXTUPOLE MAGNETS IN STORAGE RINGS

Ishaan Mishra
CLASSE, Cornell University, Ithaca NY 14853
mishrai@rose-hulman.edu

Abstract

Varying a sextupole's strength in a storage leads to changes in the orbit, phase function, and tune of a particle beam. From the difference orbit with respect to a baseline orbit with the sextupole turned-off, horizontal, vertical, quadrupole, and skew quadrupole kick differences are recorded. Due to the quadratic dependence of sextupole kicks, these recorded values are used to measure the beam size at the sextupole in the reference scan. In this paper, sextupole calibration factors and horizontal offsets with respect to the reference are integrated into the simulation software to increase the accuracy of this measurement method. Furthermore, we analyze data collected over multiple runs at the Cornell Electron-positron Storage Ring through 2021 and 2022, and present the most comprehensive dataset of the beam size measurements by analyzing the sextupole kicks on the beam.

INTRODUCTION

Background

The Cornell Electron-positron Storage Ring (CESR) is an X-ray synchrotron source of circumference 768m. CESR accelerates positrons of 1 GeV to 6 GeV using 81 dipole magnets, 114 quadrupole magnets, and 76 sextupole magnets. CESR operates as a high-energy X-ray synchrotron source [1]. Till 2008, CESR also operated as an electron-positron collider, which facilitated high energy particle physics with the CLEO detector [2].

In storage rings, dipole magnets are used to bend the beam trajectory. quadrupole magnets focus the beam bunch based on the principle of strong focusing to prolong the lifespan of the beam, while sextupoles magnets impart corrective kicks to account for higher order effects. It is shown in the next section that there is a beam-size dependence of these sextupole kicks. Taking advantage of this property, a novel method of measuring the particle beam size at the sextupoles has been developed by Crittenden et al. in [3] and [4], on which progress is reported.

Theory

A discussion of the magnetic field properties that enable this novel method of beam size measurement in storage rings has been detailed in this section. As a beam of high-energy particles are accelerated through quadrupole magnets, particles get differing focusing kicks due to the fact that the momenta of the particles deviate from the nominal particle momentum. This is analogous to chromatic aberration in classical optics [5]. Since particles in the beam bunch travel along dispersive trajectories described by the equation below, corrective kicks which depend on the particle's transverse position are required.

$$x_D(s) = D(s)\frac{\mathrm{d}p}{p_0} \tag{1}$$

Sextupole magnet kicks are dependent on the transverse position, with field strength described by the equations below. A representation of the effect of a sextupole magnet on off-momentum particles is shown in Fig.1. The sextupole field

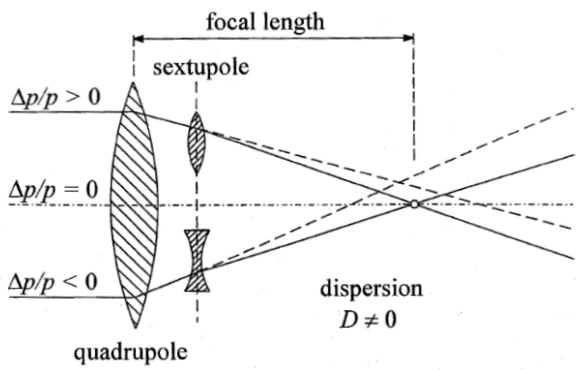

Figure 1: Representation of sextupole correction [5]

strength in a sextupole is described by the equations

$$\begin{aligned} B_y &= \frac{1}{2}B_y''(X_0^2 - Y_0^2) \\ B_x &= B_y'' X_0 Y_0 \end{aligned} \tag{2}$$

where X_0 and Y_0 are horizontal and vertical transverse beam position with respect to the sextupole center, and B_y'' is the second derivative of the magnetic field with respect to x.

The particle density of the beam are described by the Gaussian distribution

$$\rho(x) = \frac{1}{2\pi\sigma_x} \exp(\frac{-(x)^2}{2\sigma_x^2}) \tag{3}$$

The average force experienced by this beam in 1 dimension is given by

$$\begin{aligned} <F_x> &= q_0 B_y'' \int_{-\infty}^{\infty} x^2 \rho(x - X_0) \mathrm{d}x \\ &= q_0 B_y'' (X_0^2 + \sigma_x^2) \end{aligned} \tag{4}$$

For a single particle undergoing a sextupole horizontal kick,

$$\mathrm{d}x' = \frac{-q_0 l B_y''}{2P_0} (X_0^2 - Y_0^2) \tag{5}$$

where

$$k_2 = \frac{q_0 B_y''}{P_0} \tag{6}$$

Following the same process in Eq. 3-4 for both transverse dimensions, the sextupole horizontal kick with respect to a change in the sextupole strength $\mathrm{d}k_2 l$ on a Gaussian distribution of particles can be derived.

$$\mathrm{d}x' = \frac{1}{2} \mathrm{d}k_2 l (Y_0^2 + \sigma_y^2 - X_0^2 - \sigma_x^2) \tag{7}$$

The vertical dipole kick is given by

$$\mathrm{d}y' = \mathrm{d}k_2 l \, (X_0 + \mathrm{d}x) \, (Y_0 + \mathrm{d}y) \tag{8}$$

The normal quadrupole kick $\mathrm{d}k_1 l$ (also referred to as $\mathrm{d}b_1$) is given by

$$\mathrm{d}b_1 = \mathrm{d}k_1 l = \mathrm{d}k_2 l (X_0 + dx) \tag{9}$$

Thus, we can rewrite Eq. 7

$$2 \, \mathrm{d}x' = \mathrm{d}k_2 l \left[\left(\frac{\mathrm{d}y'}{\mathrm{d}k_2 l} \right)^2 \left(\frac{\mathrm{d}k_1 l}{\mathrm{d}k_2 l} \right)^{-2} + \sigma_{\mathrm{Y}}^2 - \left(\frac{\mathrm{d}k_1 l}{\mathrm{d}k_2 l} \right)^2 - \sigma_{\mathrm{X}}^2 \right] \tag{10}$$

These quantities are differences, not differentials. The equations are exact; there is no expansion. Assuming initial $k_2 l = 0$ and including all terms,

$$\sigma_{\mathrm{X}}^2 - \sigma_{\mathrm{Y}}^2 = -2 \, \frac{\mathrm{d}x'}{\mathrm{d}k_2 l} + \left(\frac{\mathrm{d}y'}{\mathrm{d}k_2 l} \right)^2 \left(\frac{\mathrm{d}k_1 l}{\mathrm{d}k_2 l} \right)^{-2} - \left(\frac{\mathrm{d}k_1 l}{\mathrm{d}k_2 l} \right)^2 \tag{11}$$

Including only terms linear in $\mathrm{d}k_2 l$, this gives,

$$\sigma_{\mathrm{X}}^2 - \sigma_{\mathrm{Y}}^2 = -2 \, \frac{\mathrm{d}x'}{\mathrm{d}k_2 l} + Y_0^2 - X_0^2 \tag{12}$$

The skew quadrupole kick gives us another way to measure Y_0.

$$\mathrm{d}a_1 = \mathrm{d}k_2 l (Y_0 + dy) \tag{13}$$

CALCULATION OF BEAM SIZES

Data Collection

Phase, orbit, and beta measurements of 6 GeV positrons in CESR were made through 2021 and 2022. These values were recorded at 100 locations by Beam Position Monitors (BPMs) and Digital Tune Trackers [6] that record data in separate phase files. One of the 76 sextupole's strength is varied, and the beam motion is recorded in a phase file. A scan consists of multiple phase files in which one sextupole magnet's strength is varied. For each scan, there must be at least 4 unique sextupole strengths so that linear fits with error can be made. One of the strength values is $k_2 l = 0$ (Sextupole is turned off). 68 scans have been recorded which have at least 4 sextupole strengths, and $k_2 l = 0$. Most scans have at least 3 phase files for each strength setting, which are averaged during the data analysis to reduce random error. A schematic of CESR's BPMs is shown in Fig. 2.

For this 6 GeV runs of CESR, the coupling factor used to calculate the vertical beam size is 2.7%. The horizontal emittance is $2.765 \times 10^{-8} m$, and the energy spread is 8.208×10^{-4}.

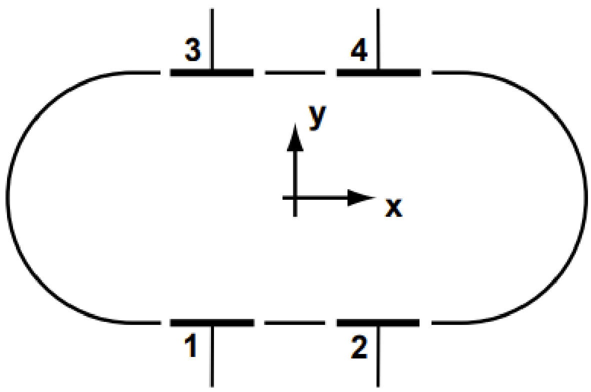

Figure 2: Schematic of a Beam Position Monitor in CESR [7]

CesrV Optimization

The scan information collected gives us information of the orbit, phase function and tune at the BPMs. The kick analysis described in this paper requires beam information at the sextupoles. CesrV ("Virtual CESR") is a multifunctional program which uses the Bmad library [8] to simulate changes of the orbit, phase, etc. of a beam at any element within CESR. It inputs a phase file and iteratively optimizes the attributes of ring elements for a simulated beam to match the data collected at the BPMs. Thus, we can extrapolate beam optics at the center of the sextupole magnet.

The Levenberg-Marquardt algorithm [9] is used by CesrV, which is an optimization algorithm used for non-linear least square fits. The program minimizes the merit function, which is a weighted sum of the square of the data and model values.

First, the CesrV program reads the reference phase file (phase file where $k_2l = 0$), and sets all the quadrupole and dipole kicks to fit the simulated phase and orbit data with the measured values. This model is then considered the "baseline". The program then reads the phase file with the sextupole turned on, and optimizes the difference orbit using only the horizontal dipole kick, vertical dipole kick, quadrupole kick, and skew quadrupole kick at the sextupole.

Twiss Analysis

An established method for beam size measurements in storage rings is by using the beta function(β), emittance(ϵ), energy spread(η), and dispersion(d). The beam size(σ) based on this method is calculated in Eq. 12.

$$\sigma = \sqrt{\beta\epsilon + (\eta \mathrm{d})^2} \tag{14}$$

These values at the sextupole are found using a CesrV simulation.The CesrV optimization gives us values of beta, eta, dispersion, which gives us expected beam sizes.

The final goal of the kick analysis is to accurately match the beam size measured through the calculations made in this section. Fig. 3 shows beam sizes calculated from the optics for all sextupoles when the sextupole strength $k_2l = 0$.

Calibration

There is systemic error in the software computer units (CU) and the actual sextupole strength (dk_2l) due to changes made in CESR's sextupole architecture in 1988. This requires correction calibration factors for the CesrV simulation. The calibration factors for all 76 sextupoles are calculated

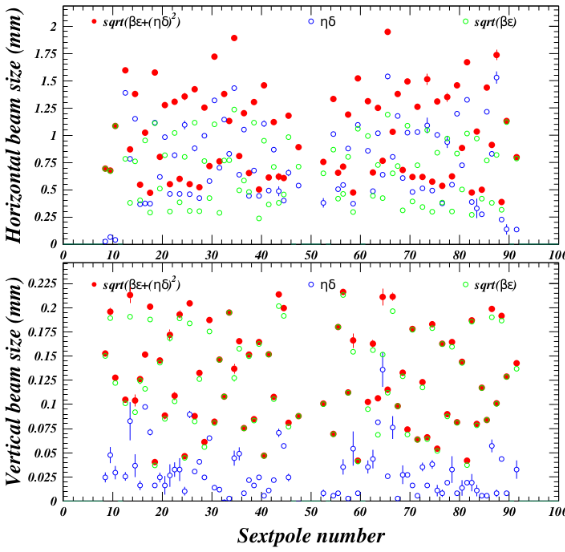

Figure 3: Horizontal and vertical beam sizes at each of the 76 sextupoles have been shown in red points. The contribution of the beta function value and emittance is shown in green, while the dispersion and energy spread values are plotted in blue.

from the beta-weighted horizontal and vertical tune shifts, described in [4]. The tune shift values are calculated after shaking the beam around the reference orbit and recording the slope of the linear term of the tune shift plotted against the beam position. The calibration factors for the sextupole magnets were added to the CesrV simulations used in this paper.

Sextupole offsets

The sextupole magnet centers are not perfectly aligned with the reference orbit (defined by the quadrupole magnet center) in CESR. Each sextupole center is offset from the reference orbit by a different value. Since the magnitude of the kicks depend on the position of the beam with respect to the center of the sextupole, it is necessary to account for the offset of the sextupoles in CESR from the expected center in the CesrV model. In [4], Crittenden et al. measure the horizontal sextupole offsets with respect to the reference orbit by measuring the horizontal and vertical tune shifts when the beam is located at different horizontal positions, as described in the subsection above. The horizontal offset which corresponds to the point on the line of best fit where the tune shift is zero is taken as the horizontal offset. Offset values for all 76 sextupoles were added to the CesrV optimization program to increase the accuracy of the model.

Kick Analysis

In this analysis only the linear terms are considered as the contribution of the non-linear terms can be neglected as seen in Fig 4, where the normal and skew quadrupole kicks, horizontal and vertical dipole kicks are plotted against the sextupole strength.

Using CERN's Physics Analysis Workstation (PAW) software, linear and non-linear terms are fitted for each of these plots, such that $\chi^2/NDF = 1$, which gives the fit error. Thus, we can find the horizontal and vertical positions of the center of the beam with respect to the reference orbit from the linear terms of the slopes db_1/dk_2l and da_1/dk_2l respectively. The plots of the skew quadrupole kick and vertical kick give us two redundant methods to determine the vertical position of the positron beam. The value of the beam vertical position is taken as the error-weighted average of the skew quad term da_1/dk_2l, and the vertical dipole term, dy'/dk_2l. Finally, the difference of the squares of the horizontal and vertical beam sizes is found using Eq. 11.

A sample calculation of the beam size using the kick analysis has been shown here. From the linear terms shown in Fig. 4, db_1/dk_2l gives us the horizontal beam position $X_0 = 1.021 \pm 0.018$ mm. Using this X_0 value, Y_0 can be determined from $dy'/dk_2l = X_0Y_0$, as well as directly from the slope of the linear term of da_1/dk_2l; The weighted average gives us $Y_0 = 1.848 \pm 0.119$ mm. Finally, these values and $dx'/dk_2l = -0.796 \pm 0.191\mu\text{rad/m}^{-2}$ are used Eq. 11, $\sigma_X^2 - \sigma_Y^2 = -2\,\frac{dx'}{dk_2l} + Y_0^2 - X_0^2$. For the 6 GeV run of CESR, the vertical beam width is approximately 1/20 of the horizontal beam size, given by the coupling factor of 2.7% for the emittance. The horizontal beam size is calculated to be 1.993 ± 0.146 mm.

Of the 68 scans, 30 gave real beam size measurements. The results of the kick analysis for these 30 scans and the corresponding analysis from the Twiss analysis are given in Table 1. Data of the remaining 38 scans with non-real beam sizes is listed in Table 2 in Appendix A. For scans with $dx'/dk_2l > 0$, it is multiplied by -1, so that $-2dx'/dk_2l > 0$

ERROR ANALYSIS

While the calibration factors and offsets make the beam size values more accurate, work still needs to be done to understand the sources of error, which result in imaginary or unrealistic beam sizes that do not match the expected

Table 1: Real beam kick data, compared with beam size calculated in Twiss analysis

Scan	Sext.	Kick $\sigma_x(mm)$	Twiss $\sigma_x(mm)$
32	34W	7.984 ± 0.162	1.893 ± 0.137
36	38W	2.464 ± 0.13	1.305 ± 0.085
39	41W	1.224 ± 0.202	0.612 ± 0.152
40	42W	1.171 ± 0.264	1.119 ± 0.108
42	44W	2.96 ± 0.049	0.606 ± 0.2
44	47W	2.73 ± 0.101	0.892 ± 0.088
45	47E	3.563 ± 0.106	0.756 ± 0.101
46	45E	4.709 ± 0.038	1.332 ± 0.07
47	44E	0.185 ± 0.332	0.657 ± 0.18
50	41E	0.776 ± 1.516	0.475 ± 0.166
52	38E	2.114 ± 0.119	1.313 ± 0.103
54	36E	0.628 ± 0.216	1.251 ± 0.106
128	35E	0.831 ± 0.266	0.765 ± 0.211
57	32E	1.253 ± 0.54	1.378 ± 0.098
58	31E	2.737 ± 0.207	0.681 ± 0.133
59	30E	3.225 ± 0.192	1.493 ± 0.074
60	29E	2.094 ± 0.116	0.618 ± 0.178
61	28E	1.976 ± 0.332	1.26 ± 0.064
62	27E	0.998 ± 0.1	0.617 ± 0.123
63	26E	3.186 ± 0.204	1.514 ± 0.066
64	25E	0.456 ± 0.313	0.575 ± 0.183
65	24E	2.77 ± 0.1	1.308 ± 0.054
66	23E	1.202 ± 0.428	0.536 ± 0.163
67	22E	3.376 ± 0.074	1.35 ± 0.09
68	21E	0.359 ± 0.219	0.623 ± 0.165
69	20E	3.349 ± 0.201	1.459 ± 0.081
72	17E	0.234 ± 0.544	0.473 ± 0.187
74	15E	2.363 ± 0.404	0.5 ± 0.117
75	14E	2.18 ± 0.248	1.436 ± 0.084
76	13E	0.756 ± 0.146	0.912 ± 0.199
78	11E	1.276 ± 0.105	0.388 ± 0.192
79	10AE	1.607 ± 0.204	1.132 ± 0.129
82	10W	2.176 ± 0.139	0.675 ± 0.196
83	12W	0.855 ± 0.008	1.595 ± 0.105
84	14W	2.005 ± 0.16	1.38 ± 0.104
86	34W	3.408 ± 0.232	1.893 ± 0.137
88	19W	1.879 ± 0.121	0.802 ± 0.145
89	20W	2.275 ± 0.155	1.277 ± 0.088
90	21W	2.501 ± 0.142	0.551 ± 0.172
91	22W	3.275 ± 0.042	1.307 ± 0.109
93	24W	3.304 ± 0.128	1.356 ± 0.047
95	25W	2.192 ± 0.124	0.552 ± 0.205
96	26W	4.078 ± 0.048	1.421 ± 0.088
97	30W	3.136 ± 0.093	1.72 ± 0.082
98	13W	1.947 ± 0.057	0.87 ± 0.213
99	34W	2.034 ± 0.184	1.893 ± 0.137
100	14W	1.874 ± 0.076	1.38 ± 0.104
101	34W	1.993 ± 0.146	1.893 ± 0.137
102	15W	0.602 ± 0.168	0.545 ± 0.126

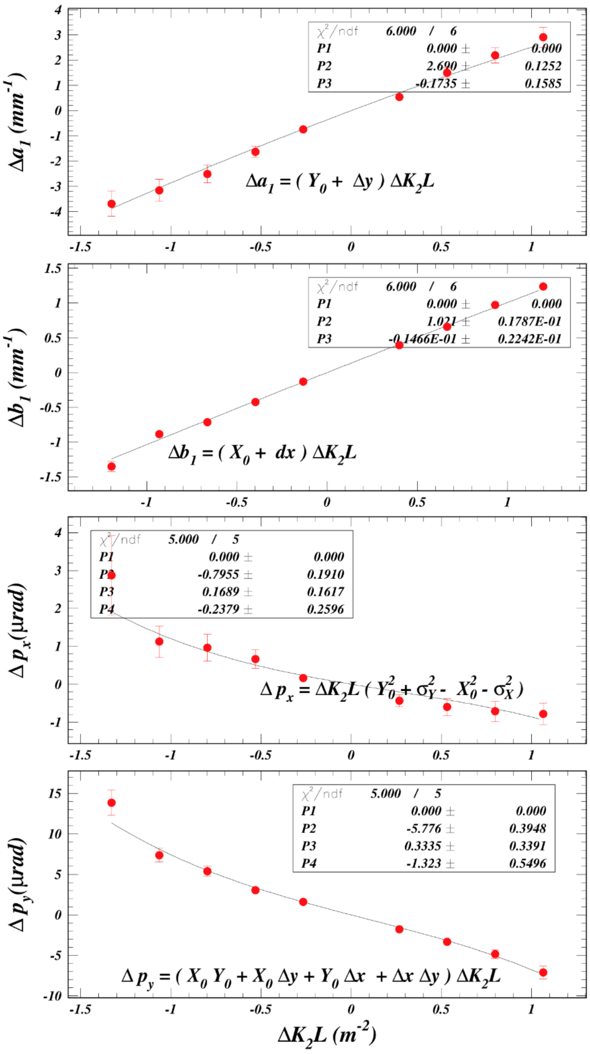

Figure 4: Kick analysis plots

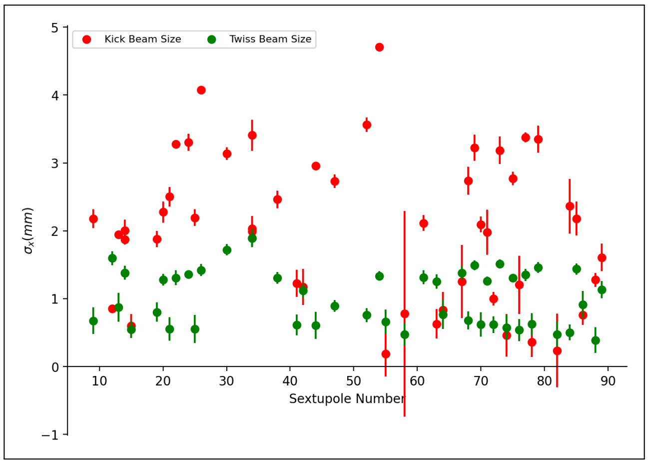

Figure 5: 49 real beams plotted with the benchmark values

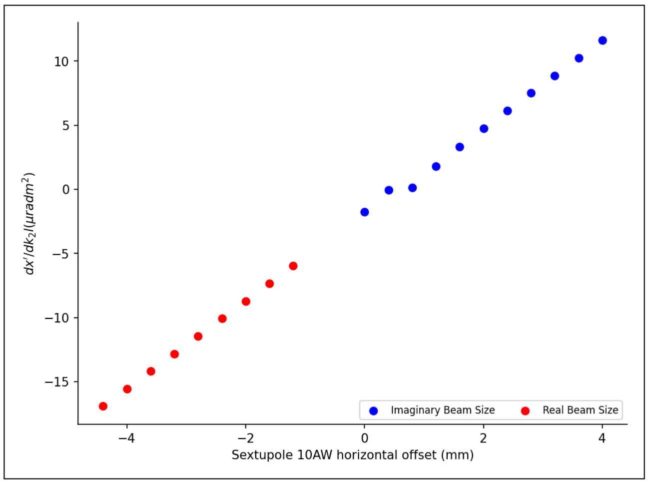

Figure 6: dx'/dk_2l plotted against the horizontal sextupole offset

values from the Twiss analysis. It was found during the kick analysis that the simulation $\mathrm{d}x'/\mathrm{d}k_2l$ value varies greatly with the sextupole horizontal offset. The other kick slopes only had minor differences. The CesrV optimization was run for Sextupole 10AW (Scan 23) with varying horizontal offsets. The $\mathrm{d}x'/\mathrm{d}k_2l$ values have been plotted against the offset in Fig. 6. This linear dependence needs to better understood, especially since none of the other three slopes were affected. The square of the beam size is negative at the actual calibration-calculated offset of 1.633 mm, resulting in an imaginary beam size.

The relative error of the beam size varies, but generally has increased accuracy compared to past iterations of the beam size kick analysis done without the addition of the calibration constants or offset values. For example, the sample kick analysis calculation in this paper has a relative error of 7.3%, compared to 26% in [4].

The dependence of the beam size on $|dx'/dk_2l|$ is expected to be linear based on Eq. 12. However, n Fig. 7 it can be seen that there are nonlinear contributions that have not yet been accounted for in the kick analysis. Moreover, when $\frac{\mathrm{d}x'}{\mathrm{d}k_2l} > 0$ and $X_0^2 > Y_0^2 + 2|\frac{\mathrm{d}x'}{\mathrm{d}k_2l}|$, the beam is imaginary.

Further studies into the effects of nonlinear terms on the kick analysis are required.

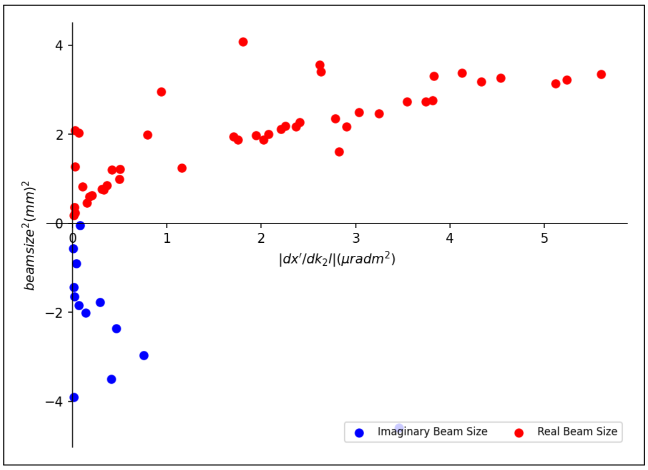

Figure 7: σ_x^2 plotted against $|dx'/dk_2l|$

CONCLUSION

In this paper, the theory of the novel method of measuring a storage ring's beam size by varying the sextupole strengths is reported on. Initially, the beam sizes at each sextupole are calculated with the CesrV simulation software, using the measured values of the beta function, emittance, energy spread, and dispersion. The sextupole calibration factors and sextupole horizontal offsets with respect to the reference orbit were incorporated into the CesrV simulation to increase the accuracy of the model. Beam sizes of 68 scans were calculated using the novel sextupole kick analysis method, and the results presented. The problem of imaginary beam sizes still persists. However, certain common characteristics of the real and imaginary beam positions and angles were identified, which may indicate that there are limitations to this beam size measurement method - that accurate, real beam sizes cannot be measured for the entire phase space of the beam. Moreover, while this preliminary data has accurate beam sizes, they do not always match with the expected beam sizes calculated using the Twiss method. Thus, the sources of error still need to be better understood. This project was a success as its goals - including the offset and calibration factors, and exploring the sources of error - was completed, and all the available CESR scans were analyzed.

ACKNOWLEDGMENTS

I thank James Crittenden and Suntao Wang for their mentorship during this REU. Their constant feedback and direction given are what made this project possible. Insights by Georg Hoffstaetter and David Sagan helped solve challenges faced during this project. I am grateful for this opportunity provided by Matthias Liepe and Jim Alexander who organized this REU at CLASSE. This research was funded by NSF award PHY-2150125 in Accelerator Physics and Synchrotron Radiation Science.

REFERENCES

[1] B.W. Batterman, "CHESS-the Cornell High Energy Synchrotron Source," in *Nuclear Instruments and Methods 172.1/2*, 172.1/2 (1980): 21-23.

[2] K. Berkelman; E.H. Thorndike, "Physics at the Cornell Electron Storage Ring," in *Annual Review of Nuclear and Particle Science 59* (2009), 297-317.

[3] J. Crittenden *et al.*, "Measurement of Horizontal Beam Size Using Sextupole Magnets," in *Proc. IPAC'21, Campinas, Brazil, May 2021, pp. 802–804.* (2021), Paper MOPAB254.

[4] J. Crittenden *et al.*, "Progress on the Measurement of Beam Size Using Sextupole Magnets", in *Proc. IPAC'22,Bangkok, Thailand, June 2022, pp.550–552.* (2022), Paper MOPOTK040.

[5] K. Wille. "The physics of accelerators: an introduction", *Clarendon Press.* (2000)

[6] R.E. Meller; M.A. Palmer. "Digital Tune Tracker for CESR," in *Proc. IPAC'11, New York, NY.* (2011), 504-506

[7] D. Sagan, et al. "Betatron phase and coupling measurements at the Cornell Electron/Positron Storage Ring," in *Physical Review Special Topics-Accelerators and Beams 3.9*, (2000): 092801.

[8] D. Sagan, "Design and Applications of the Bmad Library for the Simulation of Particle Beams and X-rays." in *11th International Computational Accelerator Physics Conference, Rostock-Warnemünde, Germany,* (2012).

[9] D.W. Marquardt, "An algorithm for least-squares estimation of nonlinear parameters," in *Journal of the Society for Industrial and Applied Mathematics 11.2.* (1963), 431-441.

APPENDIX A: IMAGINARY BEAM SIZE DATA

In this section, a compilation of the kick analysis data for scans which led to "imaginary beam sizes" are presented.

Table 2: Imaginary beam size scans

Scan No.	Sextupole No.	$\sigma_x^2(mm^2)$
23	10AW	-4.595 ± 0.328
33	35W	-17.399 ± 1.402
34	36W	-2.013 ± 0.522
35	37W	-1.429 ± 0.19
37	39W	-3.496 ± 0.696
38	40W	-15.735 ± 0.794
43	45W	-8.859 ± 0.347
51	40E	-13.747 ± 0.822
53	37E	-0.04 ± 1.059
70	19E	-0.895 ± 0.4
71	18E	-6.96 ± 1.002
73	16E	-1.848 ± 0.182
77	12E	-2.009 ± 0.594
81	9AW	-2.357 ± 0.304
85	10AW	-2.969 ± 0.132
87	33W	-3.903 ± 0.6
92	23W	-0.562 ± 0.012
94	33E	-1.64 ± 0.074
103	16W	-1.771 ± 0.539